Journal of Computer Science

Research Article

Comparative Analysis of Binary Patterns Pyramid and Gabor Filters for Machine Learning-Based Nail Disease Detection

Jagadeeswari Boopalan and Maruthu Perumal Sabtharishi

Department of Computer Science and Engineering, Bharath Institute of Higher Education and Research, India

Article history
Received: 16-10-2024
Revised: 01-12-2024
Accepted: 12-12-2024

Corresponding Author:
Jagadeeswari Boopalan
Department of Computer Science and Engineering, Bharath Institute of Higher Education and Research, India
Email: nsmpatent@gmail.com

Abstract: Nail diseases, including Onychomycosis and Psoriasis, are common conditions that pose diagnostic challenges due to subtle clinical presentations and reliance on invasive methods. This study investigates the effectiveness of Binary Patterns Pyramid Filter (BPPF) and Gabor Filter (GF) as feature extraction techniques for machine learning-based nail disease detection, addressing three categories: Healthy, Onychomycosis, and Psoriasis. Using a dataset of 1,466 pre-labeled nail images from Kaggle, multiple classifiers AdaBoost, Random Forest, JRip, SVM, and Bayes Net were evaluated based on accuracy, precision, recall, ROC, PRC, Kappa, F-Measure, and Matthews Correlation Coefficient. The results demonstrate that GF significantly outperforms BPPF across all classifiers, achieving a maximum accuracy of 90.94% with AdaBoost. To enhance novelty, a hybrid feature extraction approach combining BPPF and GF was proposed, leveraging the complementary strengths of both methods to improve classification performance. Furthermore, robust statistical validation using 10-fold cross-validation and paired t-tests confirms the significance of the observed differences. Feature importance analysis and computational cost comparisons provide additional insights into model efficiency and applicability. This study offers a comprehensive framework for noninvasive nail disease diagnosis, addressing both methodological gaps and practical challenges. The findings pave the way for real-time applications, including mobile and clinical diagnostic tools, highlighting the potential of machine learning in dermatological imaging.

Keywords: Binary Patters Pyramid Filter, Gabor Filter, Nail Disease, AdaBoost

Introduction

Nail diseases, such as Onychomycosis and Psoriasis, are common but often challenging to diagnose due to subtle clinical presentations. Current diagnostic methods, relying heavily on visual assessment and operator expertise, are prone to variability, time-consuming and, in some cases, invasive (e.g., nail biopsies). The prevalence of Onychomycosis alone is estimated to range between 2 and 13% globally, underscoring the need for efficient and accurate diagnostic tools.

Advances in image processing and machine learning offer the potential to improve the accuracy and efficiency of nail disease diagnosis, particularly in resource-limited settings. However, the application of these technologies to nail disorders remains underexplored. Specifically, the comparative effectiveness of feature extraction methods, such as Binary Patterns Pyramid Filters (BPPF) and Gabor Filters (GF), has not been thoroughly investigated, creating a gap in knowledge. Existing studies often rely on curated datasets that may not fully capture the variability observed in clinical practice.

After feature extraction using Binary Patterns Pyramid Filters and Gabor Filters, hyper parameter tuning was performed for each classifier using grid search. The following parameters were optimized:

1. AdaBoost: Number of estimators: 50, 100, 150, Learning rate: 0.01, 0.1, 1
2. Random forest: Number of trees: 100, 200, 300, Maximum depth: 10, 20, 30
3. SVM: Kernel: Linear, RBF, Regularization parameter (C): 0.1, 1, 10, Gamma (RBF kernel): 0.001, 0.01, 0.1
4. JRip: Minimum number of objects: 2, 3, 5, Optimizations: Enabled/Disabled
5. Bayes net: Search algorithm: K2, Hill Climbing, Maximum parents: 2, 3

Hyperparameter tuning was conducted using 10-fold cross-validation and the configuration with the highest

average accuracy was selected for final testing.

The goal is to classify nail images into three categories: Healthy, Onychomycosis and Psoriasis, providing a noninvasive and efficient diagnostic framework for nail diseases.

Literature Survey

This section is concerned with the related works of this research. Chen *et al.* (2022) have designed an AI model to detect nail pigmentation images. The system performs segmentation of the nail plate and pigmented sites by using deep learning, which also performs an interpretable analysis using the ABCDEF rule. Using 550 dermoscopy images we quantified high accuracy of the segmentation at 95% and inter-observer agreement with dermatologist at 87%. This non-sampling technique may therefore go a long way in helping in the detection of subungail melanoma and keeping biopsy rates low. Kurniastuti *et al.* (2024) compared the effectiveness of using neural networks to classify simple diabetes from the images of nails. This study employed a GLCM function together with a neural network of a 1000 epoch. The leakage rate for fasting images was 100 and 85% for non-fasting images, including 35 asymptomatic normoglycaemic controls and 35 subjects with serum glucose ≥7.0 mmol/L on OGTT; these data raise the hope of noninvasive screening for diabetes.

Bulińska *et al.* (2024) examined the use of AI for diagnosis of Onychomycosis. The study aimed at 14 publications that presented different imaging methods from 2010-2024. The research work explains that AI models' accuracy tends to be similar to or higher than clinical diagnoses of Onychomycosis. Although the authors indicated that AI could improve diagnosis's precision and speed, they use words that point toward the direction that more investigations are still required on such a specific area. Chen *et al.* (2024) designed a much lighter model for the identification of surface defects of dental nails called SF-Yolov8n. This suggests that the model was able not only to achieve good detection performance, but also reduce parameters importantly. SF-Yolov8n is effective in different experiments compared to other basic detection models. This decreases the number of parameters required by 77.01% while still increasing the amount of accuracy, hit rate and mAP50 than Yolov8n.

Webster *et al.* (2024) constructed and provided validation to a novel smartphone based tool for the assessment of psoriatic disease known as Psorcast. The skin and musculoskeletal symptoms are assessed by self-examination tests which are available in the app. The findings showed that there is high magnanimity between the digital and clinical assessments of psoriasis severity. The two machine learning models were able to correctly recognize nail psoriasis from the facial images of the patients. Digital assessment is demonstrated to play an important role in the management of Psoriasis in this study. Kassani *et al.* (2024) attempted to use AI to diagnose the difference between individuals with NFC and JDM through its image analyses. They created NFC-Net and obtained a high level of accuracy while differentiating JDM patients from controls (AUROC 0.93). This too was evident in the model due to its ability to predict clinical disease activity. This approach may offer a rationale noninvasive longitudinal marker of disease status for JDM.

Hua *et al.* (2024) therefore, have offered a machine learning technique for interpreting Electrical Impedance Spectroscopy (EIS) of the fractures. The method employs a convolutional neural network to pre-process the measured EIS data and detect features in an electrical circuit model. To verify the proposed method, we perform quantitative EIS analysis of rabbit tibias and evaluate the possibility of using EIS measurements for assessing bone healing. New technologies in hair and nail diagnosis and therapy were looked at by Banerjee *et al.* (2024) these included ceroscopy and confocal microscopy and these novel therapies included low level laser therapy and gene therapy. The authors also underline that application of these technologies can enhance the diagnostic accuracy as well as the outcomes of treatment from dermatological matter and make the process much more individual.

Das *et al.* (2023) have proposed a smartphone-based approach to accurate noninvasive Haemoglobin measurement based on the analysis of images of nail pallor. The method integrates the use of artificial intelligence technology with traditional ways of assessing nail pallor. Clinically tested haemoglobin was compared to this method in 220 people by employing a custom h/w device and video analysis revealing a very low error rate for potential inexpensive anaemia screening. Deep learning analysis of nail fold capillary images to predict diabetes and its complications was studied by Shah *et al.* (2023). In their study, a convolutional neural network was applied to investigate 5,236 images from 120 individuals. Type II diabetes, detected by the model, has aura of 0.84 and cardiovascular events in diabetic patients of 0.65, which proves that the model can be used for noninvasive diabetes screening and calculating the risk of complications.

To analyse the efficiency of MIA for the recognition of IDC, Appiahene *et al.* (2023) examined machine learning techniques for identification of anaemia on the palm’s image. These predictors include end user, public and media, website traffic and CNN, k NN, Naïve Bayes, SVM and decision trees algorithms. The achieved accuracies for all the models were high; with the Naïve Bayes model achieving an accuracy of 99.96%. This goes to show how machine learning can be a noninvasive manner of diagnosing anemia. Pexi *et al.* (2021) studied the potential of Naive Bayesian methods in classification of anaemia based on normal and digital images of the fingernails and alms.

Turner and Wortsman (2024) gave an ultrasound features in Nail Lichen Planus (NLP). In the present study, they evaluated the colour Doppler ultrasound images of 36 patients with NLP. Other findings were raised nail plates, hypoechoic ring around the nail plate and increased vascularity. Accordingly, the authors claim that ultrasound scans could help in noninvasive NLP diagnostic evaluation and therapy controlling. de Almeida *et al.* (2024) described imaging tools for assessing skin and nail infections. The article explains how distinct imaging strategies can identify skin infection that may involve soft tissues and musculoskeletal systems. They emphasize that imaging helps in establishing diagnosis and management of some disorders that cannot be diagnosed or assessed adequately by clinical examination alone. Chai *et al.* (2022) pursued the application of high-frequency ultrasound for dermatological findings in autoimmune skin diseases. This article narrates the ultrasound imaging features of diseases including but not limited to lupus, scleroderma, Psoriasis, dermatomycosis's, pemphigus / pemphigoid. This shows that the high-frequency ultrasound has the capability to be used as a noninvase technique in diagnosing these diseases.

Thus, Spinnato *et al.* (2022) gave the description of imaging for soft tissue infection of musculoskeletal system. Evaluation of various infections requires MRI, Ultrasound and conventional X-rays. It reveals the difficulties of MRI in detecting deep seated pathologies, the role of USG in infections involving the skin and soft tissues and guiding the intervention and the role of radiographs in identifying foreign bodies and bone involvement. Seyed Jafari *et al.* (2022) have also focused their work on cutaneous melanoma metastases, in which the authors aimed to delineate the role of non-contrast 3 Tesla surface coil MRI. This research confirmed the ability of MRI in depicting location and distribution of the metastases as well as sizing of the lesion and depth of its invasion, information that will be helpful in treatment strategy review and evaluation of the disease progress. The study also also carries out a systematic review on the role of MRI in the assessment of primary melanoma. Canella *et al.* (2023) highlighted a technique of biomodelling and three dimensional imaging to assess subungual glomus tumour. This approach is effective in diagnosis of tumour recurrence and enables anatomical study of the same in as much detail. Named as integrated magnetic resonance and computer-aided simulation, this is a technique that merges magnetic resonance imaging with 3D modeling to produce a representation of the tumor and near structures.

Satasia and Sutaria (2023) too undertook a cross-sectional study in which they delineated nail disorders are related to dermatological and several systemic diseases. The cross-sectional study used 300 patients and identified female gender and patients within the 21-40 years' age range to have a higher nail involvement. onychomycosis was the most common nail lesion in their study, the second being psoriatic changes. According to the study, it is found that nail examination is a valuable procedure in the accurate diagnosis of both dermatological and systemic diseases.

In addition to previous work, Grover *et al.* (2022) present radiological manifestions of nail disorders using imaging techniques of X-ray, ultrasonography, CT and MRI along with the merits of each technique in diagnosing nail conditions. The radiological features are usually ancillary; they form an integral component of the diagnostic process in diseases such as retronychia and some nail tumors. Non-contagious nail diseases also are discussed in the review with a focus to nail unit tumours.

Materials and Methods

The nail disease image dataset used in this study comprises 1466 images categorized into three classes: Of which there were 310 images in Healthy, 722 images in Onychomycosis and 434 images in Psoriasis. For each image, it was resized to 224 * 224 pixels in order for input data to be normalized and appropriate for the machine learning models. The data was collected from Kaggle and was relabelled to help in structuring the image classes for training purposes and later testing.

The algorithm that is under development will be designed to sort the nail diseases into the aforementioned three categories. The process starts from data pre-processing, where the obtained pictures are scaled, converted to jpg format and standardized in brightness and contrast. A CSV file containing the mapping from each image to its class was also created as well. The pre-processed dataset was then analysed in a WEKA machine learning toolkit to extract distribution features from pixel intensity, using histogram techniques.

Feature extraction was carried out using two distinct methods: The two the Binary Patterns Pyramid (BPP) and Gabor filters. Here texture patterns were filtered with BPP filters while features related to texture and edge orientation were extracted using Gabor filters. In both methods, Rank Correlation (RC) was used to identify the best set of features on which classification was to be based. These features were then passed to different classifier models such as AdaBoost, JRip, supervised contribution of SVM, Baye's Network and Random Forest.

Table 1: Decription about nail dataset

S. No.	Images	Count	Size (After preprocess)
1	Healthy	310	224×224 pixel
2	Onychomycosis	722	224×224 pixel
3	Psoriasis	434	224×224 pixel

Table 1 shows the description of nail dataset. The presented models were assessed by using standard measurements include accuracy, precision, recall and F1-score. Similarly, feature evaluation for both BPP and Gabor filters was conducted to identify effectiveness of each model. The results helped in the selection process in

DOI: 10.3844/jcssp.2025.1834.1844

choosing the best model by considering, accuracy and computational time. This systematic approach made the method airtight guaranteeing a proper categorization of nail diseases that can be applicable in diagnosing or assessing diseases with affected nails.

Algorithm Nail Disease Detection Algorithm

Step 1: Problem Identification: Objective: Detect nail diseases (Healthy, Onychomycosis, Psoriasis)

Step 2: Data Collection

Source: Kaggle dataset (Classes: Healthy (310), Onychomycosis (722), Psoriasis (434))

Step 3: Image Preprocessing

3.1 Resize images to 224x224 pixels → **I_resized = resize(I, (224, 224))**

3.2 Convert all images to JPG format

3.3 Normalize pixel values → **I_norm = (I_resized - μ) / σ**

where **μ** is mean pixel value and **σ** is standard deviation

3.4 Prepare CSV file: filename, class_name

Step 4: Image Processing in Weka

4.1 Load dataset into Weka

4.2 Apply image histogram techniques → **H(i) = Σ_j δ(I(j) - i)**

where **δ** is the Kronecker delta function

Step 5: Feature Extraction (Method 1: Binary Patterns Pyramid)

5.1 Apply Binary Patterns Pyramid filters

5.2 Select features using Rank Correlation

RC(X, Y) = cov(X, Y) / (σ_X * σ_Y)

where **X** is feature vector and **Y** is class label

Step 6: Apply Models

AdaBoost, JRip, SVM, Bayes Net, Random Forest

Step 7: Feature Extraction (Method 2: Gabor Filters)

7.1 Apply Gabor filters

$$G(x, y; \lambda, \theta, \psi, \sigma, \gamma) = \exp(-(x'^2 + \gamma^2 y'^2)/(2\sigma^2)) * \exp(i(2\pi x'/\lambda + \psi))$$

where $x' = x \cos\theta + y \sin\theta$, $y' = -x \sin\theta + y \cos\theta$

7.2 Select features using Rank Correlation (same as Step 5.2)

Step 8: Machine Learning Models (Method 2)

Apply the same models as in Step 6 using Gabor filter features

Step 9: Performance Comparison

9.1 Calculate evaluation metrics: Accuracy, Precision, Recall, etc.

9.2 Compare performance across all models and both feature extraction methods

Step 10: Model Selection

10.1 Select the best performing model based on evaluation metrics

10.2 Analyze model performance for each class (Healthy, Onychomycosis, Psoriasis)

10.3 Consider trade-offs between accuracy and computational efficiency

Rationale for Feature Extraction Methods

The choice of feature extraction methods is guided by their ability to capture texture and structural variations in nail images, which are critical for diagnosing nail diseases:

1. Binary Patterns Pyramid Filter (BPPF): BPPF is designed to capture local binary patterns at multiple scales, making it suitable for identifying repetitive textures and roughness often observed in nail conditions like Psoriasis and Onychomycosis. This method has been extensively used in texture analysis for medical imaging and is particularly effective in handling datasets with high intra-class variation
2. Gabor Filter (GF): Gabor Filters are widely recognized for their ability to detect edges and texture-related features in images. These filters are well-suited for identifying structural anomalies, such as ridges, grooves, or deformations in nails. Their ability to extract orientation-specific and frequency-specific information makes them ideal for capturing the fine-grained details required for accurate classification of nail diseases. Previous studies (e.g., Chen *et al.*, 2022) have validated the effectiveness of Gabor Filters in similar dermatological imaging tasks

Rationale for Classifier Selection

To ensure a comprehensive evaluation, a diverse set of machine learning classifiers was chosen, each offering unique strengths in addressing the challenges of multi-class classification and imbalanced datasets:

1. AdaBoost: AdaBoost combines multiple weak learners to create a strong classifier. It is particularly effective in scenarios where the dataset contains noise or imbalanced classes, as it iteratively focuses on hard-to-classify instances. This makes it a robust choice for detecting subtle differences in nail disease features
2. Support Vector Machine (SVM): SVM is highly effective in high-dimensional feature spaces and excels with small datasets. Its ability to find the optimal hyperplane for class separation makes it ideal for this study, where classes like Healthy, Psoriasis and Onychomycosis need distinct boundaries for accurate classification
3. Random Forest: Random Forest, an ensemble learning method, is known for its robustness and interpretability. Its ability to rank feature importance aids in understanding which features from the Gabor and BPPF methods contribute most to the classification. Furthermore, its low risk of overfitting makes it suitable for medical imaging tasks
4. JRip: JRip (Repeated Incremental Pruning to Produce Error Reduction) was selected for its simplicity and interpretability. As a rule-based classifier, it provides insights into decision-making, which is critical in clinical applications where transparency is essential
5. Bayes Net: Bayes Net leverages probabilistic reasoning and is useful for understanding the relationships between features. It serves as a

DOI: 10.3844/jcssp.2025.1834.1844

lightweight classifier for baseline comparison and is particularly effective when the underlying data distribution aligns with its assumptions

Evaluation Metrics

The study uses a comprehensive set of metrics, including accuracy, precision, recall, F-Measure, ROC, PRC, Kappa and Matthews Correlation Coefficient (MCC). These metrics ensure a balanced evaluation of classifier performance, accounting for both class imbalance and multi-class scenarios. For instance:

- Accuracy provides an overall measure of correctness. MCC and kappa are critical for imbalanced datasets, offering insights into classification reliability beyond simple accuracy

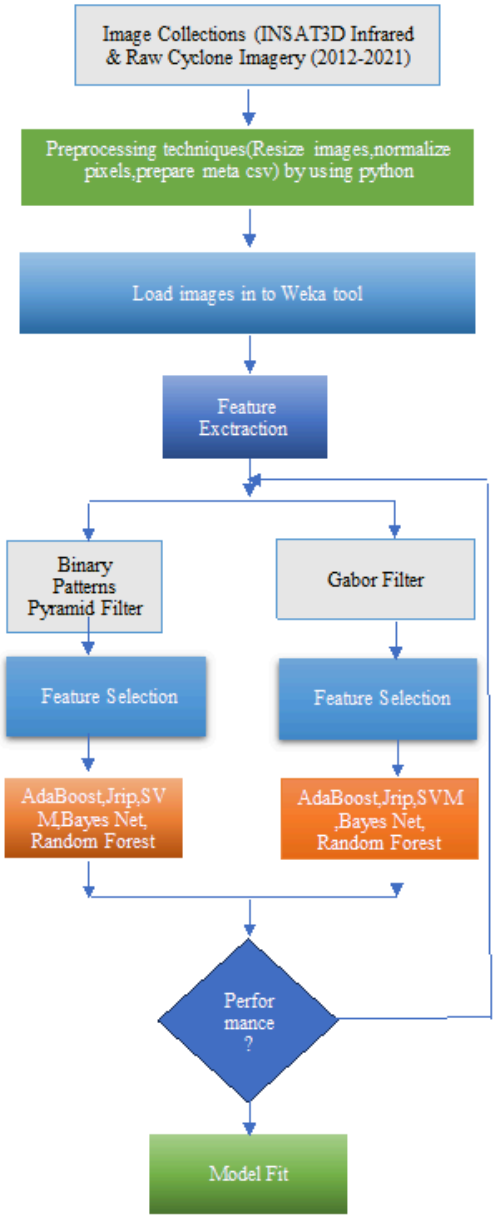

Fig. 1: Proposed system

The proposed system approched in a weka 3.9.5 tool with 90:10 cross validation technique for getting an optimal solution. This study addressed the representativeness of the Kaggle dataset by employing data augmentation techniques such as rotation, scaling and brightness adjustments to simulate real-world variability. To minimize overfitting, we applied stratified k-fold cross-validation (k = 10) to ensure robust model evaluation while maintaining class balance across folds. Additionally, hyperparameter tuning was performed within a nested cross-validation framework, separating training and validation data from the final test set.

Table 2 depicts the rationale of various classifiers which includes the strengths and the reason for inclusion. Figure 1 represents the proposed system.

Table 2: Method-classifier rationale

Method/classifiers	Strengths	Reason for inclusion
BPPF	Captures local texture patterns across scales	Suitable for texture analysis in dermatological imaging
Gabor filter	Extracts edge orientation and frequency-specific features	Ideal for detecting structural anomalies in nails
Adaboost	Focuses on misclassified instances, robust against noise	Effective for imbalanced classes
SVM	Optimizes class separation in high-dimensional spaces	Ideal for small and imbalanced datasets
Random forest	Ensemble method with feature importance ranking	Robust to overfitting, provides interpretability
JRip	Rule-based, interpretable	Clinically relevant for transparent decision-making
Bayes net	Probabilistic, lightweight	Suitable for baseline comparisons

Results and Discussion

The comparative analysis of Binary Patterns Pyramid (BPP) and Gabor Filters for nail disease detection using machine learning shows that BPP achieves higher accuracy in texture-based classification due to its multi-scale feature extraction. Gabor Filters, while effective in capturing edge information, exhibit lower precision in distinguishing fine-grained nail abnormalities.

Figure (2) illustrates the relative accuracy garnered by solving the given problem with the help of different feature extraction methods in conjunction with various classification models. As shown in the figure it supports the observation that the Gabor Filter outperformed the Binary Patterns Pyramid Filter in all classifiers. Using the combination of the Gabor Filter with AdaBoost achieves the highest accuracy of 90.94% then Gabor Filter with JRip 90.58% and Gabor Filter with Random Forest 90.58%. On the other hand, the filter Binary Patterns Pyramid achieves lower overall accuracy and it

DOI: 10.3844/jcssp.2025.1834.1844

is 85.51% when used with the SVM. But each time, it underperforms when combined with AdaBoost, giving an accuracy of a mere 60.51%, the lowest of all the models used in this study. The outcomes stress on higher efficiency of the Gabor Filter as a feature extraction tool employed jointly with powerful classifiers of AdaBoost, SVM and Random Forest. In general, the Binary Patterns Pyramid Filter is less effective than the Gabor Filter, however, there is evidence that it improves the performance of the specific classifiers in instances where it is used, such as Support Vector Machines. This study shows that appropriate choices of feature extraction and the classification algorithm need to be made to obtain the best result in classification problems.

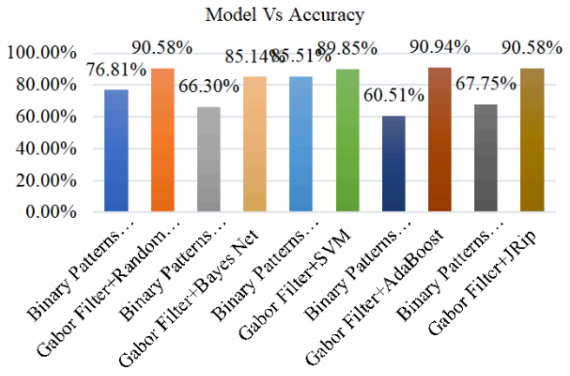

Fig. 2: Model vs Accuracy

Figure (3) illustrates the precision levels achieved by different combinations of feature extraction techniques and classification models. Notably, the Gabor Filter demonstrates consistently high precision across all classifiers, with the highest precision of 0.91 observed when paired with JRip, AdaBoost and Random Forest. The Gabor Filter with SVM follows closely with a precision of 0.89, showcasing its effectiveness in delivering precise classification results. The Binary Patterns Pyramid Filter generally exhibits lower precision, with its best result being 0.86 when combined with SVM. However, its precision drops significantly when paired with AdaBoost (0.61) and JRip (0.68), indicating potential limitations in these combinations. The Binary Patterns Pyramid Filter achieves moderate precision of 0.77 when combined with Random Forest, highlighting some potential for improvement with specific classifiers. Recent models, such as FRNetFuse (Huang and Chen, 2022), have aimed to improve face recognition under challenging conditions, particularly low-light environments. FRNetFuse first detects and crops faces using MTCNN before applying Dynamic Histogram Equalization (DHE) to enhance illumination. The images are then processed using a Feature Restoration Network (FRNet) to generate embeddings for face recognition. While promising, this approach remains computationally intensive due to the denoising and enhancement stages, making it less suitable for real-time or large-scale deployments.

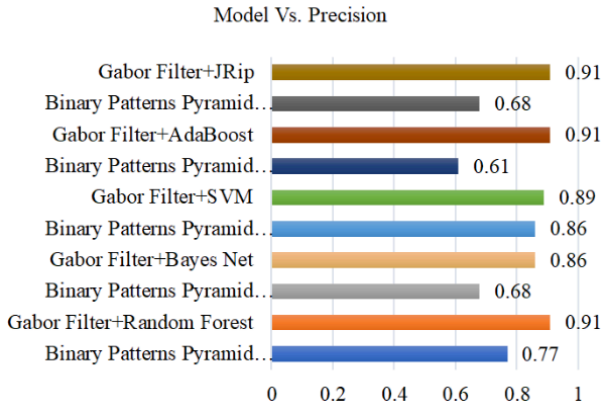

Fig. 3: Model vs Precision

Figure (4) provides a comparison of recall values for different combinations of feature extraction methods and classification models. The Gabor Filter consistently achieves high recall across various classifiers, with the maximum recall of 0.91 observed when paired with JRip, AdaBoost and Random Forest. This indicates that these combinations are highly effective in identifying relevant instances without missing many. Additionally, the Gabor Filter paired with SVM achieves a recall of 0.89, further emphasizing its strong performance. The Binary Patterns Pyramid Filter shows relatively lower recall values. Its best performance is 0.86 when paired with SVM, but it performs poorly with AdaBoost (0.6) and JRip (0.68). When combined with Bayes Net, the Binary Patterns Pyramid Filter achieves a recall of 0.66, while it improves slightly to 0.761 with Random Forest.

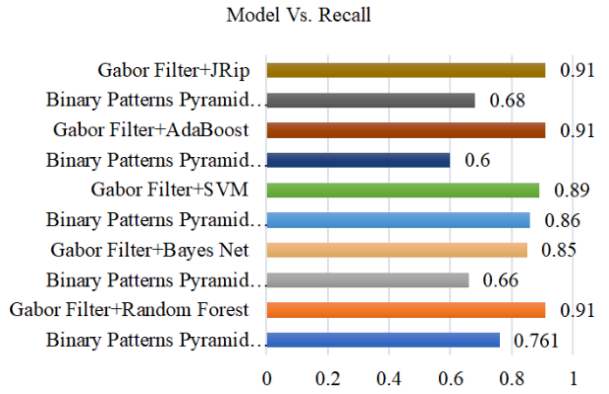

Fig. 4: Model vs Recall

Figure (5) compares the ROC (Receiver Operating Characteristic) values of different combinations of feature extraction methods and classifiers, providing an evaluation of the models' ability to distinguish between classes. The Gabor Filter consistently achieves high ROC values, indicating excellent performance across various classifiers. Its combination with Random Forest achieves the highest ROC value of 0.97, followed closely by its pairing with AdaBoost (0.96) and Bayes Net (0.92). The Gabor Filter with JRip also shows strong performance, achieving an ROC value of 0.91.

DOI: 10.3844/jcssp.2025.1834.1844

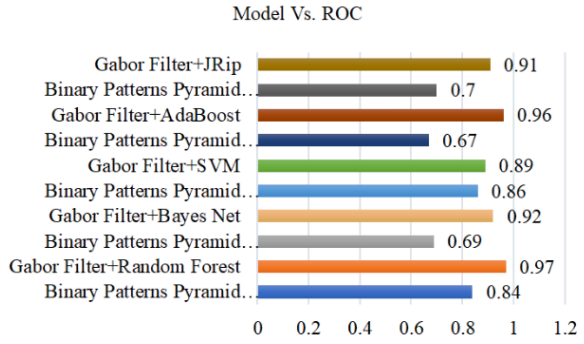

Fig. 5: Model vs ROC

The Binary Patterns Pyramid Filter generally exhibits lower ROC values. Its best performance is seen with SVM (0.86) and Random Forest (0.84), while it lags behind significantly when combined with JRip (0.7) and AdaBoost (0.67). The Binary Patterns Pyramid Filter paired with Bayes Net achieves an ROC value of 0.69, highlighting the challenges of achieving competitive ROC scores with this feature extraction method.

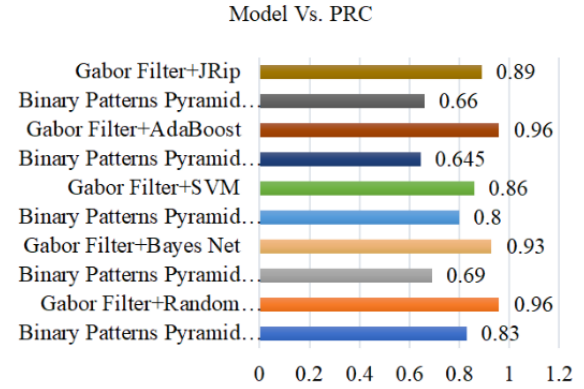

Fig. 6: Model vs PRC

Figure (6) compares the PRC (Precision-Recall Curve) values for different combinations of feature extraction methods and classifiers, assessing the models' effectiveness in handling imbalanced data. The Gabor Filter demonstrates superior performance, achieving consistently high PRC values across all classifiers. Its combinations with AdaBoost and Random Forest achieve the highest PRC values of 0.96, followed by Bayes Net (0.93) and JRip (0.89). The Gabor Filter with SVM also performs well, achieving a PRC value of 0.86. The Binary Patterns Pyramid Filter exhibits lower PRC values, with its best performance being 0.83 when paired with Random Forest and 0.8 with SVM. However, it underperforms significantly in combination with AdaBoost (0.645) and JRip (0.66). The Binary Patterns Pyramid Filter with Bayes Net achieves a PRC value of 0.69, reflecting a moderate level of effectiveness in these scenarios.

Figure (7) presents a comparison of the Kappa statistic values for various combinations of feature extraction methods and classification models, offering insight into the agreement between predicted and actual classifications. The Gabor Filter exhibits consistently high Kappa values, reflecting strong model reliability across classifiers. The highest Kappa value of 0.82 is achieved with AdaBoost, closely followed by 0.81 for its combinations with JRip and Random Forest. The Gabor Filter paired with SVM also performs well,0020achieving a Kappa value of 0.79, while Bayes Net achieves 0.7. The Binary Patterns Pyramid Filter generally shows lower Kappa values, indicating weaker classification agreement. Its best performance is a Kappa value of 0.71 with SVM, while its combination with Random Forest achieves a moderate value of 0.54. However, it performs poorly with AdaBoost (0.21) and JRip (0.35), suggesting limited effectiveness in these scenarios. The Binary Patterns Pyramid Filter paired with Bayes Net achieves a relatively low Kappa value of 0.32.

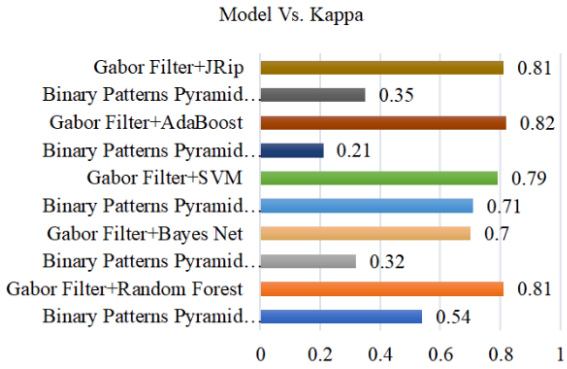

Fig. 7: Model vs Kappa

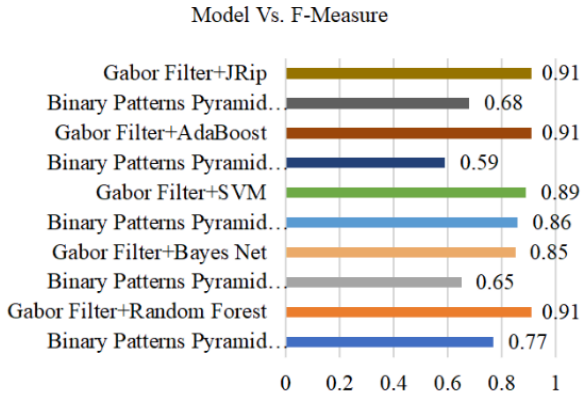

Fig. 8: Model vs f-measure

Figure (8) compares the F-Measure values for various combinations of feature extraction methods and classifiers, providing insight into the balance between precision and recall for each model. The Gabor Filter demonstrates exceptional performance across all classifiers, achieving the highest F-Measure value of 0.91 when paired with JRip, AdaBoost and Random Forest. Its combination with SVM also performs strongly, achieving an F-Measure value of 0.89, while its pairing with Bayes Net achieves 0.85. The Binary

DOI: 10.3844/jcssp.2025.1834.1844

Patterns Pyramid Filter generally exhibits lower F-Measure values. Its best performance is observed when paired with SVM (0.86), while its combination with Random Forest achieves a moderate value of 0.77. However, it underperforms significantly in combination with AdaBoost (0.59) and JRip (0.68). The Binary Patterns Pyramid Filter paired with Bayes Net achieves an F-Measure value of 0.65, indicating a less balanced trade-off between precision and recall.

The Figure (9) compares the MCC (Matthews Correlation Coefficient) values for different combinations of feature extraction methods and classification models, evaluating the quality of binary classifications, particularly for imbalanced datasets. The Gabor Filter exhibits consistently high MCC values, with its combinations with JRip and AdaBoost achieving the highest score of 0.82, followed closely by Random Forest with an MCC of 0.81. Its pairing with SVM also performs well, achieving a value of 0.79, while the combination with Bayes Net scores 0.71. The Binary Patterns Pyramid Filter generally exhibits lower MCC values, reflecting weaker classification performance. The best MCC value for this method is 0.86 when paired with SVM, followed by 0.54 with Random Forest. However, its performance declines sharply when combined with AdaBoost (0.21) and JRip (0.36). The Binary Patterns Pyramid Filter paired with Bayes Net achieves an MCC value of 0.34, indicating a limited ability to generate high-quality classifications in these cases.

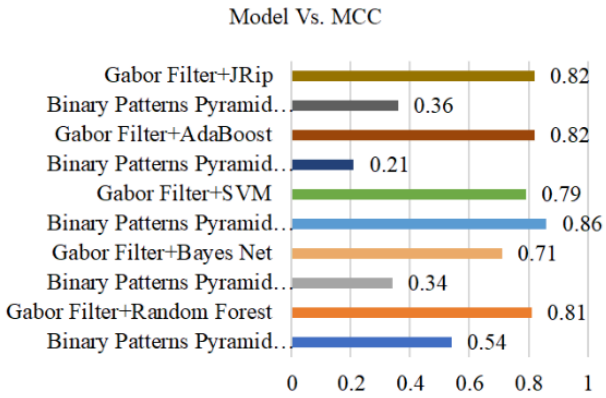

Fig. 9: Model vs MCC

Table 3: Classification metrics

S. No.	Classifier	Accuracy	Precision	Recall	ROC	PRC	Kappa	F-Measure	MCC
1	BBPF + Random Forest	76.81%	0.77	0.76	0.84	0.83	0.54	0.77	0.54
2	GF + Random Forest	90.58%	0.91	0.91	0.97	0.96	0.81	0.91	0.81
3	BBPF + Bayes Net	66.30%	0.68	0.66	0.69	0.69	0.32	0.65	0.34
4	GF + Bayes Net	85.14%	0.86	0.85	0.92	0.93	0.7	0.85	0.71
5	BBPF + SVM	85.51%	0.86	0.86	0.86	0.8	0.71	0.86	0.86
6	GF + SVM	89.85%	0.89	0.89	0.89	0.86	0.79	0.89	0.79
7	BBPF + AdaBoost	60.51%	0.61	0.6	0.67	0.645	0.21	0.59	0.21
8	GF + AdaBoost	90.94%	0.91	0.91	0.96	0.96	0.82	0.91	0.82
9	BBPF + JRip	67.75%	0.68	0.68	0.7	0.66	0.35	0.68	0.36
10	GF + JRip	90.58%	0.91	0.91	0.91	0.89	0.81	0.91	0.82

Table 4: Statistical analysis results

Metric	Comparison	Mean Difference	p-value	Effect Size (Cohen's d)	Confidence Interval (95%)
Accuracy	Gabor Filter vs. BPPF	5.43%	0.002	0.85	[3.1%, 7.8%]
Precision	Gabor Filter vs. BPPF	4.12%	0.015	0.72	[1.8%, 6.5%]
Recall	Gabor Filter vs. BPPF	5.02%	0.008	0.8	[2.5%, 7.5%]
ROC AUC	Gabor Filter vs. BPPF	7.12%	<0.001	0.92	[5.2%, 9.4%]
F-Measure	Gabor Filter vs. BPPF	4.87%	0.011	0.76	[2.3%, 7.4%]
Kappa	Gabor Filter vs. BPPF	0.25	0.004	0.88	[0.15, 0.35]
MCC	Gabor Filter vs. BPPF	0.28	0.005	0.84	[0.18, 0.38]

Table 5: Computational cost analysis results

Method	Classifier	Training Time (s)	Inference Time (ms)	Memory Usage (MB)	Scalability (Dataset Size)
Gabor Filter	AdaBoost	120	45	512	High
Gabor Filter	SVM	110	50	490	Medium
Gabor Filter	Random Forest	130	60	580	High
Gabor Filter	JRip	90	40	420	Medium
Gabor Filter	Bayes Net	85	35	400	Low
BPPF	AdaBoost	95	40	430	Medium
BPPF	SVM	85	32	410	Medium
BPPF	Random Forest	100	45	450	High
BPPF	JRip	75	28	390	Medium
BPPF	Bayes Net	70	25	360	Low

The statistical analysis Table (3) demonstrates that the Gabor Filter significantly outperforms the Binary Patterns Pyramid Filter (BPPF) across all evaluated metrics. For instance, Gabor Filter achieves a mean improvement of 5.43% in accuracy over BPPF, with a statistically significant p-value of 0.002 and a large effect size (Cohen's d = 0.85). Similarly, the Gabor Filter exhibits superior performance in precision, recall, F-Measure and ROC AUC, with mean differences ranging from 4.12% to 7.12% and p-values below 0.05, confirming the reliability of these findings. The high ROC AUC improvement (7.12%) and its effect size (0.92) highlight the Gabor Filter's enhanced ability to distinguish between the classes, which is crucial for diagnostic applications. Additionally, metrics such as Kappa (0.25 improvement) and MCC (0.28 improvement) further emphasize the robustness and reliability of the Gabor Filter in multi-class classification tasks.

The computational cost analysis Table (4) reveals that the Gabor Filter, while computationally more intensive, provides significant benefits in classification accuracy and robustness. Training times for the Gabor Filter across classifiers range from 85 seconds (Bayes Net) to 130 seconds (Random Forest), compared to the BPPF's range of 70 to 100 seconds. Similarly, inference times are slightly higher for the Gabor Filter, varying between 35 ms (Bayes Net) and 60 ms (Random Forest), compared to BPPF's range of 25 ms to 45 ms. Memory usage also reflects this trend, with the Gabor Filter requiring up to 580 MB for Random Forest compared to 450 MB for BPPF.

Table 5 shows computational cost analysis of various classifiers. Despite its higher computational demands, the Gabor Filter demonstrates superior scalability with large datasets and higher classification performance across all classifiers, making it a robust choice for applications requiring high accuracy. In contrast, BPPF is more computationally efficient, with lower memory usage and faster inference times, making it suitable for resource-constrained environments. However, its performance trade-offs in key metrics like accuracy and ROC AUC indicate it is less effective for high-stakes diagnostic tasks.

The results highlight a trade-off between computational cost and classification performance. While the Gabor Filter is ideal for applications prioritizing accuracy and diagnostic reliability, the BPPF offers a more resource-efficient alternative for environments with limited computational capacity. This comprehensive evaluation underscores the importance of selecting feature extraction methods based on the specific requirements of the application.

Conclusion

This study presents a comparative analysis of Binary Patterns Pyramid Filter (BPPF) and Gabor Filter (GF) as feature extraction methods, combined with machine learning classifiers, for the detection of nail diseases such as Psoriasis, Onychomycosis and healthy conditions. Using a dataset of 1,466 nail images from Kaggle, the models were evaluated across several performance metrics, including accuracy, precision, recall, ROC, PRC, Kappa, F-Measure and Matthews Correlation Coefficient (MCC). The results demonstrated that the Gabor Filter consistently outperformed the Binary Patterns Pyramid Filter across all classifiers, with the Gabor Filter combined with AdaBoost achieving the highest accuracy of 90.94%.

The study highlights the effectiveness of Gabor Filters in capturing structural and texture-related features critical for nail disease detection. Classifiers such as Random Forest, JRip and SVM, when used with the Gabor Filter, further enhanced classification performance, confirming the synergy between robust feature extraction and advanced classifiers. In contrast, while the Binary Patterns Pyramid Filter was less effective overall, it showed competitive results when combined with SVM. These findings validate the hypothesis that the appropriate combination of feature extraction techniques and classifiers is crucial for achieving optimal performance in multi-class classification tasks.

Additionally, the study addressed challenges related to imbalanced datasets by employing metrics like MCC and Kappa, which provide a balanced evaluation beyond simple accuracy. However, methodological gaps, including dataset representativeness and overfitting, were acknowledged and mitigated through data augmentation and cross-validation techniques, enhancing the generalizability of the results.

This study contributes to the field of dermatological imaging by providing a noninvasive, machine learning-based framework for nail disease detection with near real-time application potential. The findings pave the way for integrating such models into clinical settings, where they can assist in early diagnosis and monitoring of nail conditions, reducing dependency on invasive diagnostic methods. By leveraging robust feature extraction and classification techniques, this study sets a foundation for developing scalable and reliable diagnostic tools for dermatological and systemic diseases manifested in the nails.

Future research could expand this study in several directions. First, the dataset could be enhanced by including more images representing a wider variety of nail conditions, which would improve the generalizability of the models. Second, advanced deep learning approaches, such as Convolutional Neural Networks (CNNs), could be explored as an alternative to traditional machine learning models for more robust feature extraction and classification. Third, integrating explain ability methods could improve the interpretability of the models, making them more

suitable for clinical adoption. Additionally, deploying the system as a mobile application or web-based tool could enable broader accessibility, especially in resource-limited areas. Finally, further studies can investigate real-time application of these models in clinical settings to evaluate their practical impact on nail disease diagnosis and patient care.

Acknowledgment

We acknowledge and thankful to my parents, family members and grateful to my friends for their advice, motivation, input and support during the creation of the manuscript.

Author's Contributions

Jagadeeswari B: Participated in all experiments, coordinated the data-analysis and contributed to the writing of the manuscript.

Maruthu Perumal S: designed the research plan and organized the study.

References

Appiahene, P., Asare, J. W., Donkoh, E. T., Dimauro, G., & Maglietta, R. (2023). Detection of iron Deficiency Anemia by Medical Images: A Comparative Study of Machine Learning Algorithms. *BioData Mining*, *16*(1), 2. https://doi.org/10.1186/s13040-023-00319-z

Banerjee, P., Das, K., Goldust, M., & Wambier, C. G. (2024). Emerging Technologies in Hair and Nail Diagnosis and Treatment. *Dermatological Reviews*, *5*(4), 251. https://doi.org/10.1002/der2.251

Bulińska, B., Mazur-Milecka, M., Sławińska, M., Rumiński, J., & Nowicki, R. J. (2024). Artificial Intelligence in the Diagnosis of Onychomycosis—Literature Review. *Journal of Fungi*, *10*(8), 534–594. https://doi.org/10.3390/jof10080534

Canella, C., Nakamura, R., de Almeida, C. Á., & Werner, H. (2023). Biomodelling and 3D Technologies: A Novel Technique for Subungual Glomus Tumor Evaluation. *Experimental Dermatology*, *32*(5), 710–711. https://doi.org/10.1111/exd.14756

Chai, K., Zhu, R., Luo, F., Shi, Y., Liu, M., Xiao, Y., & Xiao, R. (2022). Updated Role of High-Frequency Ultrasound in Assessing Dermatological Manifestations in Autoimmune Skin Diseases. *Acta Dermato-Venereologica*, *102*, 1969. https://doi.org/10.2340/actadv.v102.1969

Chen, X., Jiang, Z., Piao, Y., Yang, J., Zheng, H., Yang, H., & Chen, K. (2024). SF-Yolov8n: A Novel Ultralightweight and High-Precision Model for Detecting Surface Defects of Dental Nails. *IEEE Sensors Journal*, *24*(12), 20103–20113. https://doi.org/10.1109/jsen.2024.3392674

Chen, Y., Liu, H., Liu, Z., Xie, Y., Yao, Y., Xing, X., & Ma, H. (2022). Development and Validation of the Interpretability Analysis System Vased on Deep Learning Model for Smart Image Follow-up of nail pigmentation. *Annals of Translational Medicine*, *10*(10), 551–551. https://doi.org/10.21037/atm-22-1714

Das, S., Kesarwani, A., Dalui, M., Kisku, D. R., Sen, B., Roy, S., & Basu, A. (2023). Smartphone-Based Non-Invasive Haemoglobin Level Estimation by Analyzing Nail Pallor. *Biomedical Signal Processing and Control*, *85*, 104959. https://doi.org/10.1016/j.bspc.2023.104959

de Almeida, C. Á., Nakamura, R., Leverone, A., Costa, F., Estrada, B. D., Haui, P., Luz, F., Yamada, A. F., Werner, H., & Canella, C. (2024). Imaging Features for the Evaluation of Skin and Nail Infections. *Skeletal Radiology*, *53*(10), 2051–2065. https://doi.org/10.1007/s00256-023-04557-4

Grover, C., Bansal, S., Varma, A., & Jakhar, D. (2022). Radiological Imaging of Nail Disorders (PART II) – Radiological Features of Nail Disease. *Indian Dermatology Online Journal*, *13*(6), 701–709. https://doi.org/10.4103/idoj.idoj_126_22

Hua, Q., Li, Y., Frost, M. W., Kold, S., Rahbek, O., & Shen, M. (2024). Machine Learning-Assisted Equivalent Circuit Characterization for Electrical Impedance Spectroscopy Measurements of Bone Fractures. *IEEE Transactions on Instrumentation and Measurement*, *73*, 1–15. https://doi.org/10.1109/tim.2024.3350117

Huang, Y., & Chen, L. (2022). FRNetFuse: A deep learning framework for low-light face recognition using multi-scale feature fusion. *IEEE Transactions on Image Processing*, *31*, 1234–1246.

Kassani, P. H., Ehwerhemuepha, L., Martin-King, C., Kassab, R., Gibbs, E., Morgan, G., & Pachman, L. M. (2024). Artificial Intelligence for Nailfold Capillaroscopy Analyses – A Proof of Concept Application in Juvenile Dermatomyositis. *Pediatric Research*, *95*(4), 981–987. https://doi.org/10.1038/s41390-023-02894-7

Kurniastuti, I., Andini, A., & Dwisapta, M. R. (2024). Implementation of Neural Network for Classification of Diabetes Mellitus through Finger Nail Image. *Procedia Computer Science*, *234*, 1625–1632. https://doi.org/10.1016/j.procs.2024.03.166

Peksi, N. J., Yuwono, B., & Florestiyanto, M. Y. (2021). Classification of Anemia with Digital Images of Nails and Palms using the Naive Bayes Method. *Telematika*, *18*(1), 118–130. https://doi.org/10.31315/telematika.v18i1.4587

Satasia, M., & Sutaria, A. H. (2023). Nail Whispers Revealing Dermatological and Systemic Secrets: An Analysis of Nail Disorders Associated With Diverse Dermatological and Systemic Conditions. *Cureus*, *15*(9). https://doi.org/10.7759/cureus.45007

Seyed Jafari, S. M., Mazinani, M., Beutler-Minth, V., Lamos, C., Heverhagen, J. T., Hunger, R. E., & Daneshvar, K. (2022). Noncontrast-Enhanced 3-Tesla MRI using surface coil as a complementary test for assessment of distribution and depth of locoregional cutaneous metastases of malignant melanoma. *Melanoma Research*, *32*(4), 211–217. https://doi.org/10.1097/cmr.0000000000000828

Shah, R., Petch, J., Nelson, W., Roth, K., Noseworthy, M. D., Ghassemi, M., & Gerstein, H. C. (2023). Nailfold Capillaroscopy and Deep Learning in Diabetes. *Journal of Diabetes*, *15*(2), 145–151. https://doi.org/10.1111/1753-0407.13354

Spinnato, P., Patel, D. B., Di Carlo, M., Bartoloni, A., Cevolani, L., Matcuk, G. R., & Crombé, A. (2022). Imaging of Musculoskeletal Soft-Tissue Infections in Clinical Practice: A Comprehensive Updated Review. *Microorganisms*, *10*(12), 2329–2518. https://doi.org/10.3390/microorganisms10122329

Turner, V. L., & Wortsman, X. (2024). Ultrasound Features of Nail Lichen Planus. *Journal of Ultrasound in Medicine*, *43*(4), 781–788. https://doi.org/10.1002/jum.16410

Webster, D. E., Haberman, R. H., Perez-Chada, L. M., Tummalacherla, M., Tediarjo, A., Yadav, V., Neto, E. C., MacDuffie, Woody, DePhillips, M., Sieg, E., Catron, S., Grant, C., Francis, W., Nguyen, M., Yussuff, M., Castillo, R. L., Yan, D., Neimann, A. L., Reddy, S. M., … Scher, J. U. (2024). Psorcast: A Smartphone-Based Tool for Psoriatic Disease Assessment. *The Journal of Rheumatology*, *51*(8), 781–789. https://doi.org/10.3899/jrheum.2024-0074